Modeling the Mechanics of Polymer Chains with Deformable and Active Bonds

Shawn R. Lavoie†, Rong Long‡, Tian Tang†,*

†Department of Mechanical Engineering, 10-203 Donadeo Innovation Centre for Engineering, 9211-116 Street NW, Edmonton, AB, T6G 1H9, Canada

‡ Department of Mechanical Engineering, University of Colorado at Boulder, Boulder, CO, USA 80309.

*Corresponding author E-mail: tian.tang@ualberta.ca, Phone: 780-492-5467, Fax: 780-492-2378

Abstract

The force-extension relationship of single polymer chains is an essential component underlying the development of macroscopic constitutive models for elastomers. In this work, we present a model for the force-extension relationship beyond the consideration of classical entropic elasticity, by accounting for bond deformation on the chain's backbone. Parameters in this model are mostly molecular parameters for bond stretching, bending and breaking already available in the literature, thereby limiting the parameters that need to be extracted from fitting experimental data to a minimum. In addition, an extension of the model is made to include the effects of mechanophores: molecules that react under the application of a mechanical force. This

has endowed the model with the capability of predicting mechanophore reaction as well as chain scission. The model is applied, and compared to experimental data, in a range of scenarios: reproducing the measured force-extension relationship for PDMS chains, calculating the rate dependent fracture energy of PDMS films, and predicting the force-extension relationship caused by the unfolding of mechanophore domains. For the last example it was demonstrated that this type of chains has the potential to be utilized to design elastomers with substantially enhanced strength and toughness.

1 Introduction

To capture the nonlinear mechanical behaviors of elastomers with macroscopic constitutive models, the microscopic force-extension relationship for a single polymer chain is often required[1, 2, 3]. Classically, polymer chain elasticity has been modeled by considering the change in entropy, e.g., in the freely jointed chain model[1] or the worm-like chain model[4]. Because these models only consider entropy, they exhibit a limiting extension at which the chain force becomes singular. Near this singularity such entropic models give poor predictions for the force-extension relationship which cannot match experimental measurements. These models are therefore insufficient for problems where chains are highly stretched and eventually break, such as fracture, since force-extension relationships accurate in the large extension range are needed. There has been some effort along this direction in the literature. For example, the elastic freely jointed chain model is an extension of the original freely jointed chain model, by considering the links to be elastic springs[5]. Recently, another model was presented based on minimizing the free energy of the chain which consists of entropy and the energy associated with deformation of bonds[6-7].

In fracture problems it is also desirable to be able to predict the rupture of chains that lead to damage in the vicinity of the cracks. Previously chain rupture has been modeled by using a critical bond deformation energy[6-7], or by solving kinetic equations where the rate of scission for a polymer chain is enhanced by the tensile force acting on it[4, 8, 9]. The latter was shown to be able to predict rate dependence of fracture phenomena in elastomers[9]. Fundamentally, bond rupture can be considered as a particular type of chemical reaction that occurs to a polymer chain. Other types of chemical reactions can be introduced to engineer the mechanics and rupture behaviors of a polymer chain. In particular, recently there have been strong interests towards the development of active polymer chains containing mechanophores, which could respond to mechanical force by changing color[10, 11], emitting light upon rupture[12], or increasing the chain length[13-17].

In this work, we aim at developing a comprehensive model that captures several aspects of a polymer chain under mechanical loading: its entropic elasticity, bond deformation on the backbone, kinetics of bond scission, and activation of mechanophores embedded in the chain. Parameters in the model are largely molecular parameters (e.g. Kuhn length, number of bonds) already available in literature, and additional parameters required for fitting are minimal. The model allows us to generate force-extension relationships that compare very well with experimental data for a large range of extension. It also enables the evaluation of rate-dependent fracture energy of a polymeric interface, which agrees well with experiments. Finally, using this model, we demonstrate how certain types of active polymer chains with mechanophores can be used to enhance the theoretical maximum stress and toughness at the continuum level.

The paper proceeds as follows. The formulation of the model is given in Section 2 with the generalization to include mechanophores discussed in Section 2.4. Results are presented in Section 3 which is divided to present: i) the force-extension relationship for a simple chain (in

absence of mechanophores) in Section 3.1, ii) scission of simple chains in Section 3.2, iii) the impact of mechanophores on scission in Section 3.3, and iv) chains that can increase length upon activation in Section 3.4. Conclusions are given in in Section 4.

2 Theory

2.1 Entropic elasticity

There are numerous models in the literature[1, 2, 4] which relate the tensile force on a polymer chain to its fractional extension, defined as the ratio between the chain's end-to-end distance and its contour length. An implicit assumption in these models is the chain being inextensible in that the contour length, i.e., length of the fully extended chain, is a constant. Since the chain in these models is inextensible, a force is required to increase the end-to-end distance mainly due to the decrease in configurational entropy during this process. For example, in the persistence chain model[4], a chain is idealized as N_K Kuhn segments each with Kuhn length A [18] so that the constant contour length is given by $L_c = N_K A$. The chain force-extension relationship given by this model is

$$F = \frac{k_B T}{P}\left(\frac{1}{4}(1 - r^*)^{-2} - \frac{1}{4} + r^*\right), \quad (1)$$

where F is the tensile force acting on the polymer chain, $P \approx A/2$ is the persistence length[4], k_B is the Boltzmann constant and T is the absolute temperature. The fractional extension in this equation is

$$r^* = \frac{r}{L_c}, \quad (2)$$

where r is the end-to-end distance.

The relationship in Eq. (1) is in good agreement with experimental data for fractional extension less than 0.9[4]. Above this extension, Eq. (1) predicts that the force increases abruptly and approaches infinity as r^* approaches unity (entropic locking extension), which is much higher than that observed in the experiments of single chain extension[4]. In this large extension regime ($r^* > 0.9$), force-extension relationships based on entropic elasticity do not work well due to the breakdown of the inextensibility assumption. In reality when r^* approaches one the chain will be subjected to forces large enough to significantly deform the bonds on the chain's backbone. Deformation of the bonds will allow the end-to-end distance, r, to increase beyond the contour length of the undeformed chain. This behavior will cause the force to increase more gradually with the fractional extension rather than being singular as in the entropic elasticity model[6-7].

2.2 Polymer Chain with Deformable Bonds

Consider the stretching of a polymer chain, for which a schematic is shown in Figure 1. Comparing Figure 1a) and c) as the end-to-end distance increases from its initial value $\sqrt{\langle R_o^2 \rangle}$ to the current value r, there will be less possible configurations the chain can assume which causes a decrease in entropy. Meanwhile if we compare the bonds on the chain backbone shown in Figure 1b) and d) the tensile force F causes the bonds to stretch from their initial length l_o to l, and the bond angle to decrease from initial value θ_o to θ. If we consider the geometry in Figure 1d) the contour length of the chain can be written in terms of the bond length and angle[18]:

$$L_c = N_K A = n_b l \cos\left(\frac{\theta}{2}\right), \quad (3)$$

where n_b is the number of bonds on the chain backbone. Assuming that the number of Kuhn segments N_K remains constant, Eq. (3) allows us to establish a relationship that determines how

the deformation of bonds will impact the Kuhn length and cause it to increase from its initial value of $A_o = \frac{n_b}{N_K} l_0 \cos\left(\frac{\theta_0}{2}\right)$ to the current value of

$$A = \frac{L_c}{N_K} = \frac{n_b}{N_K} l \cos\left(\frac{\theta}{2}\right).$$	(4)

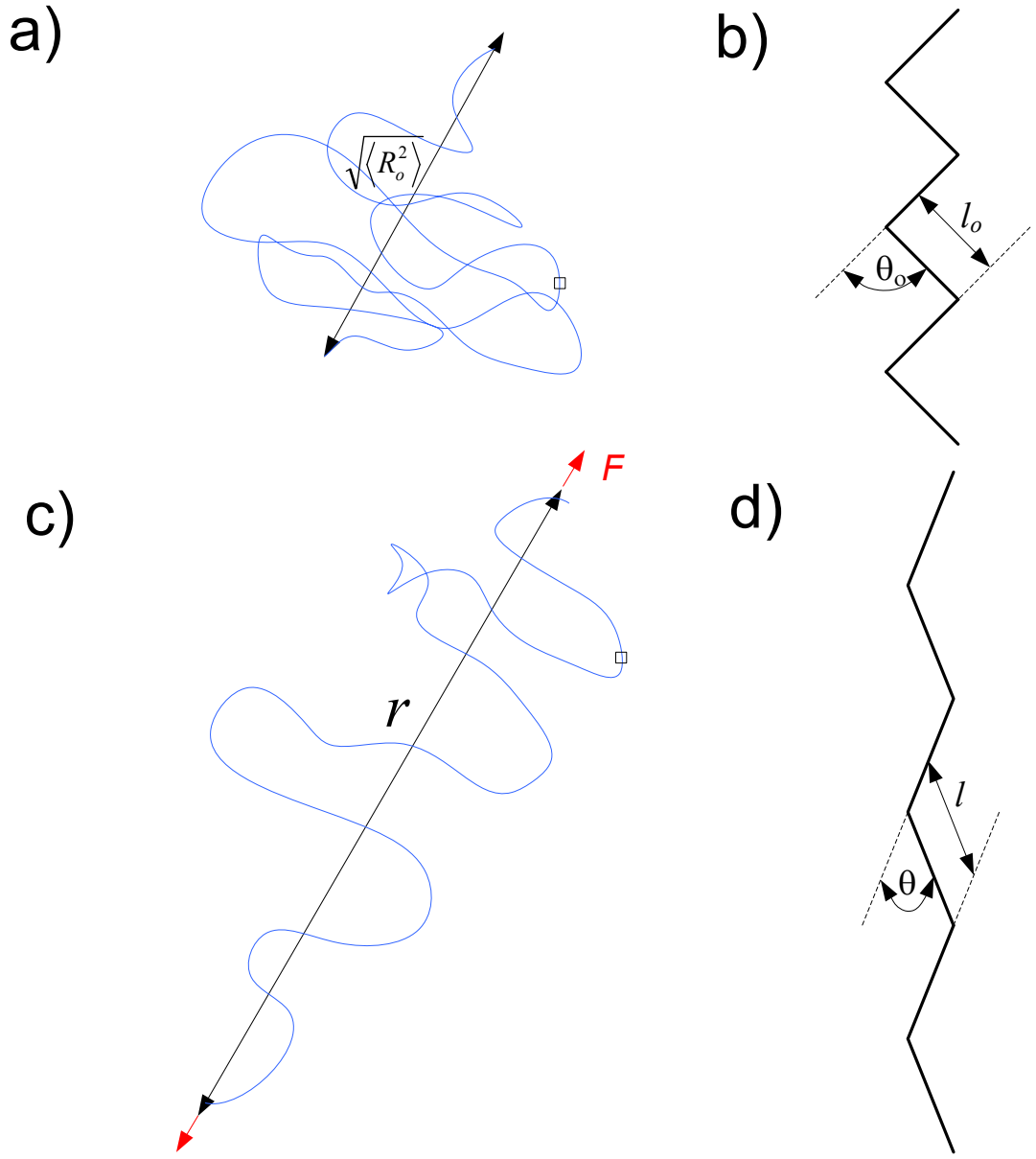

Figure 1: a) Polymer chain before stretching b) backbone bonds before stretching c) polymer chain after stretching d) backbone bonds after stretching.

In order to model the deformation of backbone bonds as the chain is stretched, we assume that the Helmholtz free energy of the polymer chain, measured relative to a completely relaxed configuration, consists of three components

$$E_{ch} = E_{ent} + n_b[E_{str} + E_{ben}], \quad (5)$$

where E_{ent} is the change in free energy arising from the decrease in configuration entropy as the chain is straightened, E_{str} is the change in internal energy (per bond) due to bond stretching, and E_{ben} is the change in internal energy (per bond) due to deformation of bond angles.

The first component in Eq. (5), E_{ent}, is obtained by integration of Eq. (1) which yields

$$E_{ent}(r^*) = \int F dr = N_K A \int F dr^* = k_B T N_K \left(\frac{1}{2}(1 - r^*)^{-1} - \frac{1}{2}r^* + r^{*2}\right). \quad (6)$$

It should be noted that the relationship presented in Eqs. (1) and (6) is merely one example of entropic chain elasticity, while the methodology discussed in this work could be applied to any other relationships. For example in the Supporting Information (Section S1) we also present relationships based upon Gaussian chains statistics[19] and Langevin chain statistics[1]. Here E_{ent} is written in terms of the fractional extension of the deformed chain i.e. $r^* = r/N_K A < 1$. Later we will show that it is more convenient to define a second fractional extension in terms of the initial Kuhn length, $r_o^* = r/N_K A_o$.

The stretching of bonds is assumed to follow a Morse potential[20], with the energy given by

$$E_{str} = D_e\left[\left(1 - e^{-\beta_s(l - l_o)}\right)^2 - 1\right], \quad (7)$$

where D_e is the dissociation energy of a bond, $l - l_o$ is the change in bond length from its equilibrium value, and β_s is a constant which controls the width of the potential. The Morse potential is used because it has a relatively simple functional form and, unlike a harmonic function, it well captures the energetics of a chemical bond from its equilibrium position to dissociation[20]. The tensile force acting on a bond can be obtained by taking the derivative of E_{str} as follows

$F_{str} = \frac{\partial E_{str}}{\partial l} = 2D_e\beta_s\left(1 - e^{-\beta_s(l-l_o)}\right)e^{-\beta_s(l-l_o)}.$	(8)

For illustration Eqs. (7) and (8), in non-dimensional form, are shown in Figure 2. It can be seen that F_{str} has a peak value of $F_{pk} = D_e\beta_s/2$ which occurs at $l_{\rm pk} - l_o = \ln 2/\beta_s$. This peak force corresponds to the maximum force that a bond can sustain before rupture, although in reality the chain can break much sooner due to thermal-fluctuation. F_{str}, the tensile force on a bond, should be distinguished from the tensile force acting on the chain, F. The relation between the two quantities will be derived later.

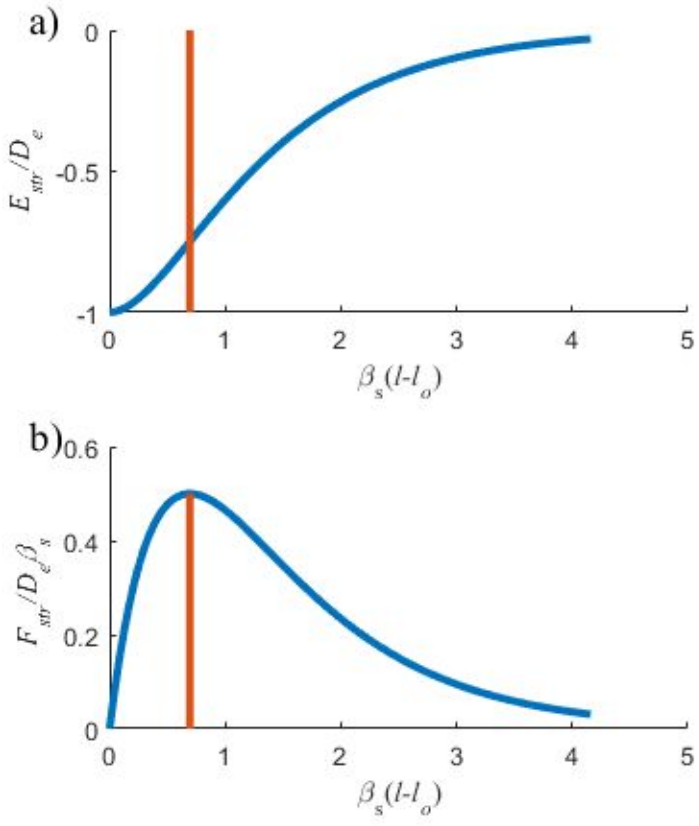

Figure 2: a) Morse potential for bond stretching b) Force obtained from the Morse potential. Orange lines mark the location of the peak value for F_{str}, and the corresponding value for E_{str}.

The deformation of a bond angle is assumed to be governed by the following potential[20]

$$E_{ben} = \frac{1}{2}k_\theta(\theta_o - \theta)^2\left[1 + k_s(\theta_o - \theta)^4\right], \quad (9)$$

where $\theta_o - \theta$ is the change in bond angle from its equilibrium value, and k_θ and k_s are constants. The bending moment can be obtained from this potential as follows

$$M = \frac{\partial E_{ben}}{\partial \theta} = k_\theta(\theta_o - \theta)\left[1 + 3k_s(\theta_o - \theta)^4\right]. \quad (10)$$

Although the energies in Eq. (5) are individually defined by Eqs. (6), (7), and (9), constraints are needed to determine compatible values of r^*, l and θ. Specifically, if the chain's end-to-end distance r is fixed, l and θ should be such that the Helmholtz free energy is minimized. Since at fixed r, $dE_{ch} = (\partial E_{ch}/\partial l)|_{r,\theta}dl + (\partial E_{ch}/\partial \theta)|_{r,l}d\theta$, this condition implies that

$$\left.\frac{\partial E_{ch}}{\partial l}\right|_{r,\theta} = 0 = \left.\frac{dE_{ent}\partial r^*}{dr^*\ \partial l}\right|_{r,\theta} + n_b\frac{dE_{str}}{dl} = \frac{dE_{ent}}{dr^*}\frac{\partial}{\partial l}\left(\frac{r}{n_b l\cos(\theta/2)}\right) + n_b F_{str}$$

which leads to

$$F_{str} = Fr^*\cos\left(\frac{\theta}{2}\right), \quad (11)$$

and

$$\left.\frac{\partial E_{ch}}{\partial \theta}\right|_{r,l} = 0 = \left.\frac{dE_{ent}\partial r^*}{dr^*\ \partial \theta}\right|_{r,l} + n_b\frac{dE_{str}}{d\theta} = \frac{dE_{ent}}{dr^*}\frac{\partial}{\partial \theta}\left(\frac{r}{n_b l\cos(\theta/2)}\right) + n_b M$$

which leads to

$$M = -Fr^*\frac{l}{2}\sin\left(\frac{\theta}{2}\right) = -F_{str}\frac{l}{2}\tan\left(\frac{\theta}{2}\right). \quad (12)$$

Using these two conditions, the tensile force acting on the polymer chain, assuming constant temperature, can now be calculated from

$$F = \frac{dE_{ch}}{dr} = \frac{\partial E_{ch}}{\partial r}\Big|_{l,\theta} + \frac{\partial E_{ch}}{\partial l}\Big|_{r,\theta}\frac{dl}{dr} + \frac{\partial E_{ch}}{\partial \theta}\Big|_{r,l}\frac{d\theta}{dr} = \frac{dE_{ent}}{dr} = \frac{dE_{ent}}{dr^*}\frac{1}{N_K A}. \quad (13)$$

2.3 Bond and Chain Parameters for Common Polymers

To use Eqs. (7) and (9) four constants need to be known. Typical values have been obtained from the literature for C-C and Si-O bonds (Table 1), which are commonly found in many elastomeric materials.

Table 1: Values of constants in bond potentials for common elastomer backbone bonds, where D_e is the dissociation energy of a bond, β_s is a constant which controls the width of the Morse potential, k_θ is the linear angular stiffness, and k_s is an additional angular stiffness which corresponds to an energy term proportional to the angular deformation to the 6th power. See Eqs. (7) and (9) for details.

Bond Type	C-C[20]	Si-O[21]
D_e (J)	6.031×10^{-19}	7×10^{-19}
β_s ($10^{10}/m$)	2.625	2
k_θ (J/rad^2)	9×10^{-19}	$3.15 - 12.42 \times 10^{-19}$
k_s (rad^{-4})	0.754	0 (potential used did not have k_s)

It is also desirable to obtain l_o, θ_o, as well as the initial Kuhn length A_o and the number of bonds per Kuhn segments n_b/N_K using existing data. Typical values for A_o and molecular weight of a Kuhn segment, M_K, are summarized in Table 2 for a variety of polymers. To determine the ratio n_b/N_K, we express the molecular weight of a chain in two different ways: $M_{ch} = N_K M_K = n_b M_b$, where M_b is the average molecular weight per backbone bond which can be calculated by

dividing the molecular weight of the repeating monomer unit M_m by the number of backbone bonds per repeating unit n_m. For example, consider PDMS where the repeating unit structure is $[-Si(CH_3)_2-O-]_n$ and it has a molecular weight of $M_m = 74.17$ g/mol. The monomer has three backbone bonds; however, two bonds are shared with adjacent monomers so these two bonds are only counted as one towards n_m which gives $n_m = 2$. Therefore, $M_b = M_m/n_m = 37.08$ g/mol. Finally, the ratio n_b/N_K, denoted by ξ, can be determined by

$$\xi \equiv \frac{n_b}{N_K} = \frac{M_K n_m}{M_m}. \quad (14)$$

To determine the equilibrium bond angle θ_o, consider the mean square end-to-end distance for a free chain (without external loading applied), which can be expressed in two ways[18]: $\langle R_o^2 \rangle = N_K A_o^2 = C_\infty n_b l_o^2$, where C_∞ is the long-chain asymptotic limit of Flory's characteristic ratio, and its values are available in the literature[18, 22] (Table 2). This leads to the following relation: $(N_K A_o)^2 = N_K C_\infty n_b l_o^2$. According to Eq. (3), the contour length of a free chain is $N_K A_o = n_b l_o \cos(\theta_o/2)$. Combining the two results we arrive at the following expression

$$\xi = \frac{C_\infty}{\cos^2(\theta_0/2)}. \quad (15)$$

Since ξ can be obtained from Eq. (14), this relation allows for the computation of θ_0. Finally, with all other parameters determined, Eq. (4) can be applied to a free chain, $A_o = \frac{n_b}{N_K} l_o \cos\left(\frac{\theta_o}{2}\right)$, to calculate the equilibrium bond length. The calculated chain parameters are shown in Table 3.

Table 2: Available material parameters for a variety of common polymers, where C_∞ is the long-chain asymptotic limit of Flory's characteristic ratio, A_o is the initial Kuhn length, M_K is the molecular weight of a Kuhn segment, M_m is the molecular weight of the repeating monomer unit, n_m is the number of backbone bonds per repeating unit, and ρ is the density.

Polymer	Monomer Structure	C_∞	A_o (Å)	M_K (g/mol)	M_m (g/mol)	n_m	ρ (g/cm^3)
Poly(dimethyl siloxane) (PDMS)[18]	$[-Si(CH_3)_2-O-]_n$	6.8	13	381	74.17	2	0.895
Poly(methyl methacrylate) (PMMA)[18]	$[-CH_2-C(CH_3)(COOCH_3)-$	9.0	17	655	100.12	2	1.13
Poly(methyl acrylate) (PMA)[22]	$[-CH_2-CH(COOCH_3)-]_n$	7.91	14.7	494.6	86.09	2	1.22
Poly(ethyl acrylate) (PEA)[22]	$[-CH_2-CH(COOCH_2CH_3)-$	9.76	18.1	710.1	100.1	2	1.13

Table 3: Calculated molecular parameters.

Polymer	$\xi = \frac{n_b}{N_K}$	θ_o (degree)	l_o (Å)
Poly(dimethyl siloxane) (PDMS)	10.27	71.11	1.56
Poly(methyl methacrylate) (PMMA)	13.08	67.92	1.57
Poly(methyl acrylate) (PMA)	11.49	67.86	1.54
Poly(ethyl acrylate) (PEA)	14.18	67.91	1.54

2.4 Active Chains with Mechanophores

Recently there have been strong interests in embedding mechanophores, molecules in which mechanical forces can trigger a reaction, onto polymer chains to produce active materials capable of emitting light upon rupture[12], changing color[10, 11], or relieving stress[16]. For example, it was shown that with the addition of certain mechanophores, sufficiently large tensile force caused the conversion of shorter monomers to longer ones[13-17], which led to a plateau in the chain force-extension relationship. The theory presented above can be extended to describe such polymer chains.

To do so, Eq. (5) must be modified to include additional contributions to the chain energy due to mechanophores. If we consider a chain that has n_1 mechanophore units in the

unconverted state and n_2 mechanophore units in the converted state, then the chain energy can be written as

$$E = E_{ent} + n_b[E_{str} + E_{ben}] + n_1E_1 + n_2E_2, \quad (16)$$

where E_1 and E_2 are the energy of one unit in the unconverted and converted states respectively. Before any force is applied $n_2 = 0$. If we denote the lengths of the unconverted and converted mechanophore units as l_1 and l_2 respectively, where $l_2 > l_1$, the contour length of the chain will be given by

$$L_c = N_K A = n_b l\cos\left(\frac{\theta}{2}\right) + n_1 l_1 + n_2 l_2. \quad (17)$$

Note that unless $n_1 << n_b$ the tabulated values discussed in the last section cannot be used to determine A_o. Instead the Kuhn length is now defined as

$$A = \frac{L_c}{N_K} = \frac{n_b l\cos(\theta/2) + n_1 l_1 + n_2 l_2}{N_K}, \quad (18)$$

and the initial Kuhn length is $A_o = \left[n_b l_0\cos\left(\theta_0/2\right) + n_1 l_1\right]/N_K$ where no force is applied on the chain and no mechanophores are triggered. The force acting on each mechanophore unit can be obtained by taking the derivative of the potential with respect to the length of the unit:

$$F_1 = \frac{dE_1}{dl_1}, \quad (19)$$

$$F_2 = \frac{dE_2}{dl_2}. \quad (20)$$

As before constraints are needed to ensure compatible values of r^*, l, θ, l_1 and l_2. Specifically, if the chain end-to-end distance r is fixed, l, θ, l_1 and l_2 should be such that the free energy is minimized. In this case, Eqs. (11) and (12) still hold, whereas two more constraints are imposed:

$$\left.\frac{\partial E_{ch}}{\partial l_1}\right|_{r,l,\theta,l_2} = 0 = \left.\frac{dE_{ent}}{dr}\frac{dr}{dr^*}\frac{\partial r^*}{\partial l_1}\right|_{r,l,\theta,l_2} + n_1\frac{dE_1}{dl_1} = -Fn_1r^* + n_1F_1$$

similarly

$$\left.\frac{\partial E_{ch}}{\partial l_2}\right|_{r,l_1} = 0 = -Fn_2r^* + n_2F_1$$

which leads to

$$F_{MP} = F_1 = F_2 = Fr^*, \quad (21)$$

where we have denoted the force acting on the mechanophore units to be F_{MP}.

Consider an example where the mechanophores upon external loading undergo a reaction in which their lengths increase by approximately 16%[13]. In this particular material[13] the entire polymer chain is made of mechanophores, so effectively $n_b = 0$ in Eq. (16). $E_1$and E_2 in Eq. (16) have been represented by quadratic functions[13] and are shown in Figure 3a). The forces calculated from Eqs. (19) and (20) are shown in Figure 3b). Here points A (at 0.948 nm) and B (at 1.099 nm) mark the lengths for the unconverted and converted mechanophore units, respectively, at which they experience zero force. The dashed line connecting C to D is a hypothetical transition, from the unconverted to the converted states, at a force of 2 nN. According to Eq. (21) the force remains constant during this transition.

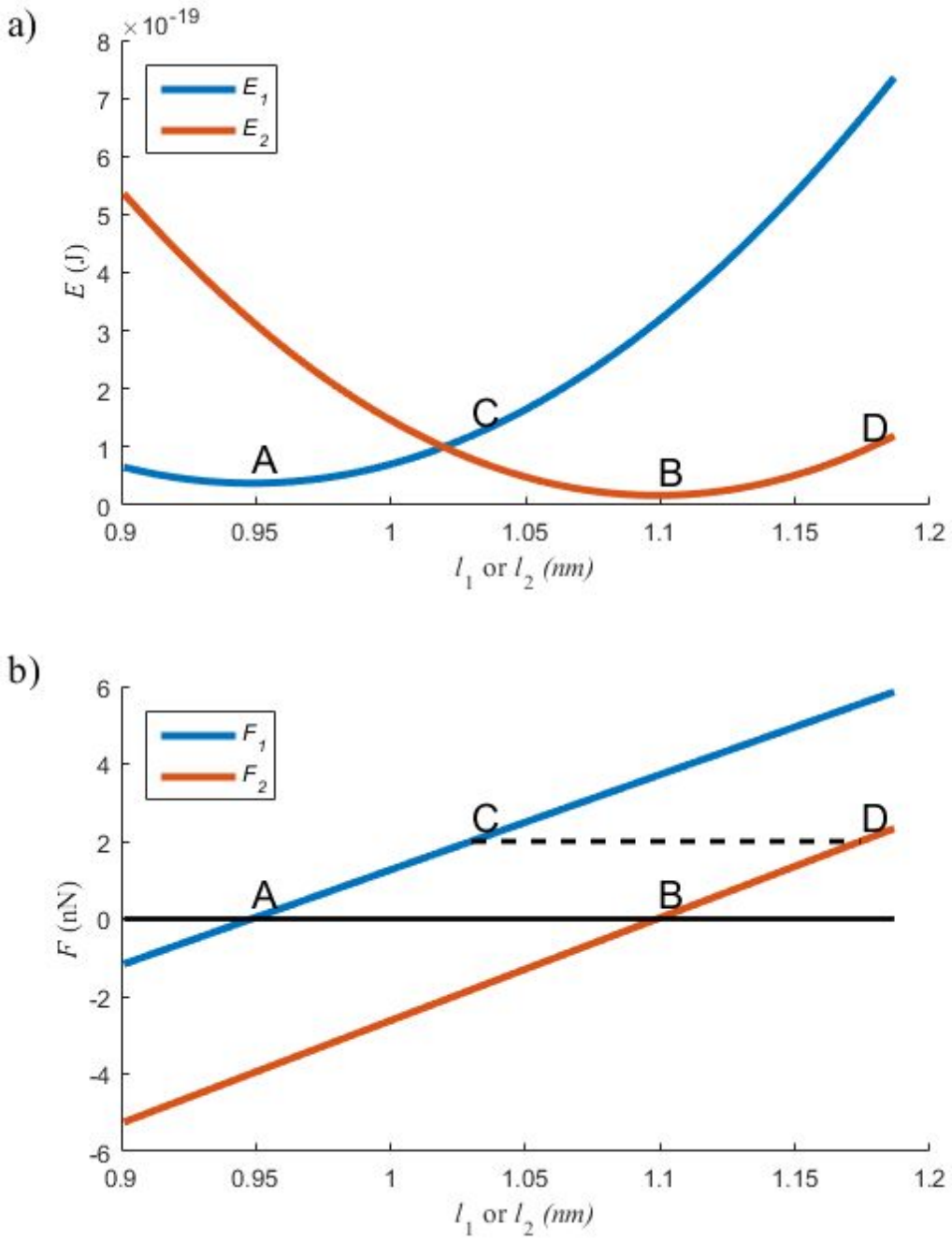

Figure 3 a) Energies of unconverted and converted mechanophore units proposed in Want et al.[13]. $E_1[kJ/mol] = 6678.6 - 1403.52l_1 + 73.99l_1^2$ corresponds to cis-syn-CL-gCFC repeating unit where l_1 is in Angstrom. $E_2[kJ/mol] = 9652.16 - 1754.9l_2 + 79.85l_2^2$ corresponds to 2-fluro-3-chloro-alkene (Z isomer) repeating unit where l_2 is in Angstrom. b) Corresponding force profiles obtained by taking the derivatives of E_1 and E_2.

2.5 Reaction Kinetics

The bonds on a polymer chain backbone can dissociate, and in some cases can re-associate, with certain reaction rates. Such reactions rates are influenced by the application of external forces. For instance, some models propose that the activation energy for bond dissociation is decreased by a term that is equal to the external force multiplied by the activation length[4, 8, 9]. A refinement to this approach is the cusp model where a mechanical force f on the bonds alters the position of the reactants which changes the activation length[14, 23]. In this model, the reaction rate k can be written as[5, 14, 23]

$$k(f) = k_o\left(1 - \frac{fx^{\ddagger}}{2\Delta G^{\ddagger}}\right)^{-2} \exp\left(\frac{fx^{\ddagger}}{k_B T}\left(1 - \frac{fx^{\ddagger}}{4\Delta G^{\ddagger}}\right)\right), \quad (22)$$

where k_o is a constant controlling the reaction rate, $\Delta G^{\ddagger}$ is the activation energy of the transition state and $x^{\ddagger}$ is the activation length of the transition state. Eq. (22) predicts a critical force[5] at which the reaction rate becomes singular:

$$f_{crit} = \frac{2\Delta G^{\ddagger}}{x^{\ddagger}}. \quad (23)$$

The reaction rate equation in Eq. (22) can be applied to describe the rupture of regular polymer bonds[5, 23], as well as the transition of mechanophores from shorter to longer lengths[13, 14]. Firstly, if we denote the fraction of surviving regular bonds (i.e., not mechanophore) as b_P then the scission of these bonds can be modeled by[3, 4, 8, 9]

$$-\frac{db_P}{dt} = n_b b k(F_{str}). \quad (24)$$

where b is the surviving chain fraction from both backbone bonds and mechanophore rupture to be defined later. To predict the rate of mechanophore reaction, we denote the unreacted fraction of mechanophores as b_{MP} so that

$$n_1 = n_0 b_{MP}, \quad (25)$$

$$n_2 = n_0(1 - b_{MP}), \quad (26)$$

where $n_0 = n_1(t = 0)$. The mechanophore reaction will be governed by

$$-\frac{db_{MP}}{dt} = n_0 b_P[b_{MP}k(F_{MP}) - (1 - b_{MP})k_R(F_{MP})], \quad (27)$$

where $k_R(F_{MP})$ denotes the rate of reverse reaction where the mechanophores transition from longer to shorter lengths; the entire equation is multiplied by b_P as mechanophore reactions are not possible on broken chains. It should have a different functional form than Eq. (22) because the reverse reaction is altered by the mechanical force differently than the forward reaction[10, 11]. In this work we focus on cases where the forward reaction dominates (i.e., mechanophore elongation upon tensile force) and the reverse reaction is negligible (i.e., $k_R(F_{MP}) \approx 0$) in Eq. (27)). The other two reaction rates $k(F_{str})$ and $k(F_{MP})$ will be governed by different constants (k_o, $\Delta G^{\ddagger}$ and $x^{\ddagger}$). In the literature these reaction rates have typically been predicted by using the polymer chain force F[3, 4, 5, 8, 9, 13, 14, 23] in Eq. (22). However, because the model presented in this work provides the force acting on the bonds F_{str} and the force acting on the mechanophores F_{MP} separately, more physical force measures can be used in predicting the reaction rates.

Now consider a bulk polymer and denote its surviving (unbroken) chain fraction as b, then the average force each chain carries is

$$F_{eff} = bF. \quad (28)$$

b can be related to b_P and b_{MP} above. For simple polymer chains (no mechanophores)

$$b = b_P. \quad (29)$$

However, if the chain also contains mechanophores which rupture after reaction, then

$$b = b_{MP} b_P, \quad (30)$$

where b_P is predicted by Eq. (24) and b_{MP} is predicted by Eq. (27) with $k_R = 0$. There are three special cases involving mechanophores for which the above equations can be simplified. In the first case, the activation of a mechanophore does not produce any change in mechanical properties. Rather b_{MP} could indicate quantities such as color change. This feature can be reproduced by letting $E_1 = E_2$ and $l_1 = l_2$, and has been previously explored in the literature[10, 11]. In the second case, the mechanophores are used as crosslinkers and the reacted state is a dissociated bond. An example of this is the bis(adamantyl)-1,2-dioxetane bisacrylate mechanophores used to crosslink elastomers[12]. Because the mechanophore is a crosslinker, there is a mechanophore on either end of the chain so $n_1 = 2$. Since $n_1 << n_b$ it is a reasonable approximation to use equations from Sections 2.1 and 2.2 rather than the more general equations presented in Section 2.4. Surviving chain fraction for this case is given by Eq. (30). This scenario is also applicable to crosslink failure which has recently been of interest[24, 25]. This case is examined in Section 3.3. In the third case the polymer chain is constructed entirely of mechanophores[13] and hence $n_b = 0$. In Section 3.4 we consider such a polymer where the activation of a mechanophore increases the contour length of the chain. The transition is reported to be permanent[15] so $k_R = 0$.

2.6 Solution Procedure

The desired output is the force-extension relationship (F vs. $r_o^* = r/N_K A_o$), $b_P(r_o^*)$, and in some cases $b_{MP}(r_o^*)$. Here we have introduced a second fractional extension in terms of the initial Kuhn length, $r_o^* = r/N_K A_o$ and all functions are solved in terms of r_o^*. This variable has been chosen because it can be related to the first invariant of the left Cauchy Green deformation tensor of the bulk material, $I_1(\underline{\mathbf{B}})$[1]. Eqs. (24) and (27) are solved using the Runge-Kutta method with adaptive step-size control[26] to obtain $b(r_o^*)$ and $b_{MP}(r_o^*)$ where r_o^* (and hence r) is increased in each step. During each step it is necessary to obtain several intermediate variables by simultaneously solving multiple equations. For a simple polymer chain (no mechanophores) Eqs. (1)-(4), (8), (10)-(12) are solved to obtain F, L_c, A, l, θ, F_{str}, M and r^*. If mechanophores are present, then Eqs. (1)-(2), (8), (10)-(12), (17)-(21) are solved to obtain F, L_c, A, l, θ, F_{str}, M, r^*, l_1, l_2, and F_{MP}.

While the procedure above is relatively efficient, there are certain applications, such as development of a constitutive model for bulk polymer based on the present single chain theory, where implementation of this iterative numerical procedure at many points in the material would be computationally costly. For this reason, we have also used curve fitting to provide simple yet accurate representations for the solutions to F in terms of r_o^* for several polymers. A summary of the fitting procedure and results is given in the Supporting Information (Section S2).

3 Results and Discussion

Representative results from the model are presented in several sections. For PDMS we compare the predicted force-extension relationship (Sections 3.1) and rate-dependent damage with experimental data extracted from literature (Sections 3.2). These chains do not have embedded mechanophores and will be referred to as simple chains. In Section 3.3 we address the

effect of crosslinking mechanophores on the damage of PEA chains. Finally, in Section 3.4 we study an active chain made entirely of mechanophore units that increase in length upon activation. Force-extension relationship predicted from the model is compared with experimental data in literature. It will be demonstrated how this type of chain could lead to improved mechanical properties in polydisperse elastomers. Necessary molecular parameters are taken from Table 1 and Table 2.

3.1 Simple Chain without bond scission

To illustrate how the chain force and bond deformation change as the fractional extension (r_o^*) is increased, several quantities for a PDMS chain are plotted in Figure 4. In Figure 4a) the force acting on the chain F (blue) and the force acting on the bonds F_{str} (red) are plotted. As expected from Eq. (11) F is slightly larger than F_{str}. In addition, for this polymer the entropic locking extension $r_o^* = 1$ is exceeded. Also, shown in the inset of Figure 4a) is the same data with the y-axis changed to a logarithmic scale. This plot highlights the difference at low chain fractional extension where the chain force is dominated by configuration entropy and the chain force is large relative to the bond force. The deformation of bond length (blue) and angle (red) as a function of r_o^* are shown in Figure 4b). When the force is small the deformation of bonds is negligible indicating the force is determined primarily by entropy. However, once a fractional extension of about $r_o^* = 0.9$ is reached sufficient force is present to cause significant bond deformation. After this point r^* changes from increasing linearly with r_o^* to asymptotically approaching 1 as shown in Figure 4c). This feature prevents the force singularity that occurs at $r_o^* = 1$ in purely entropic models.

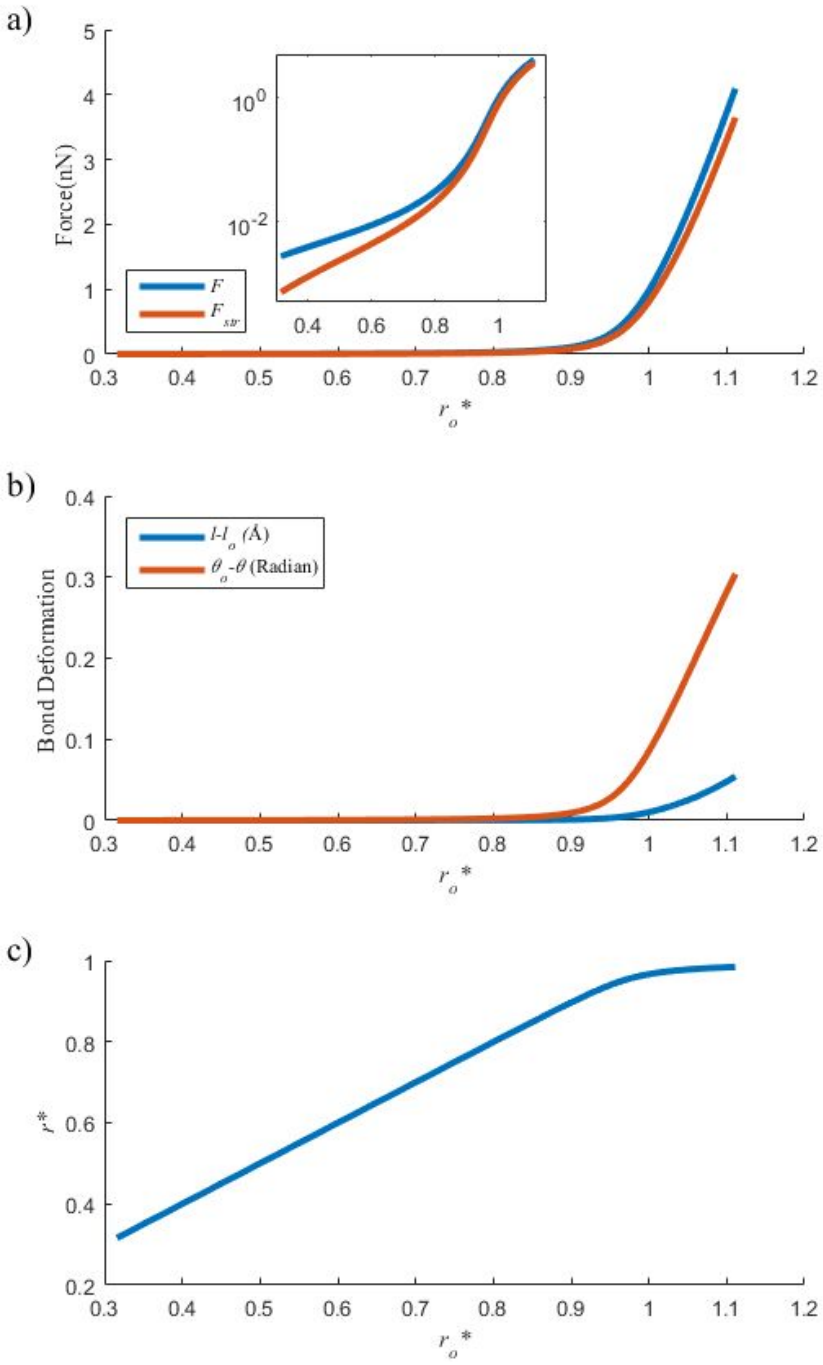

Figure 4 a) Tensile forces acting on the chain and acting on the bonds. The inset figure represent the same data with the plotted using a logarithm scale for the y-axis b) Deformation of bond length and angle plotted against r_o^*. c) r^* plotted against r_o^*. The parameters used in generating these graphs are for PDMS (Table 2) and Si-O bond (Table 1).

Without the consideration of damage, the force-extension relationship for PDMS chain is shown in Figure 5 (blue). Also shown in this figure is the relationship based purely on entropic elasticity (yellow, given by Eq. (1)). Clearly, the deformation of bonds makes the force-extension relationship considerably softer for $r_o^* > 0.9$. In Ghatak *et al*.[4], single chain extension data were presented for PDMS, and the entropic chain model was found to be able to fit the data only up to $r_o^* = 0.9$. To see if the model established here performs better in describing the force-extension relationship, the same experimental data are also shown in Figure 5. This data was obtained from atomic force microscopy (AFM) measurements which, in the raw form, is force vs. end-to-end distance *r*. When attempting to fit the data using the entropic model (Eq. (1)), two fitting parameters are needed: the Kuhn length which impacts the force magnitude, and the contour length which impacts the fractional extension. The Kuhn length obtained using this method is often much smaller than the tabulated values; for example, 0.3 nm as determined in Ghatak *et al*.[4] versus 1.3 nm tabulated in Rubenstein *et al*.[18]. In our model, the tabulated value for the Kuhn length (1.3 nm for PDMS) is directly used and the only fitting parameter is the contour length. To produce a good fit between our model and experimental data a contour length slightly shorter than that in Ghatak *et al*[4] is needed, so we have scaled up their reported fractional extensions by a factor of 1.085 in Figure 5. In the same figure we have also shown the experimental data without the scaling in fractional extension (green) as well as the fit provided in Ghatak *et al*[4] (purple) using an entropic model and a small Kuhn length of 0.3 nm. The fit was only able to match the experimental data up to the fractional extension of 0.9.

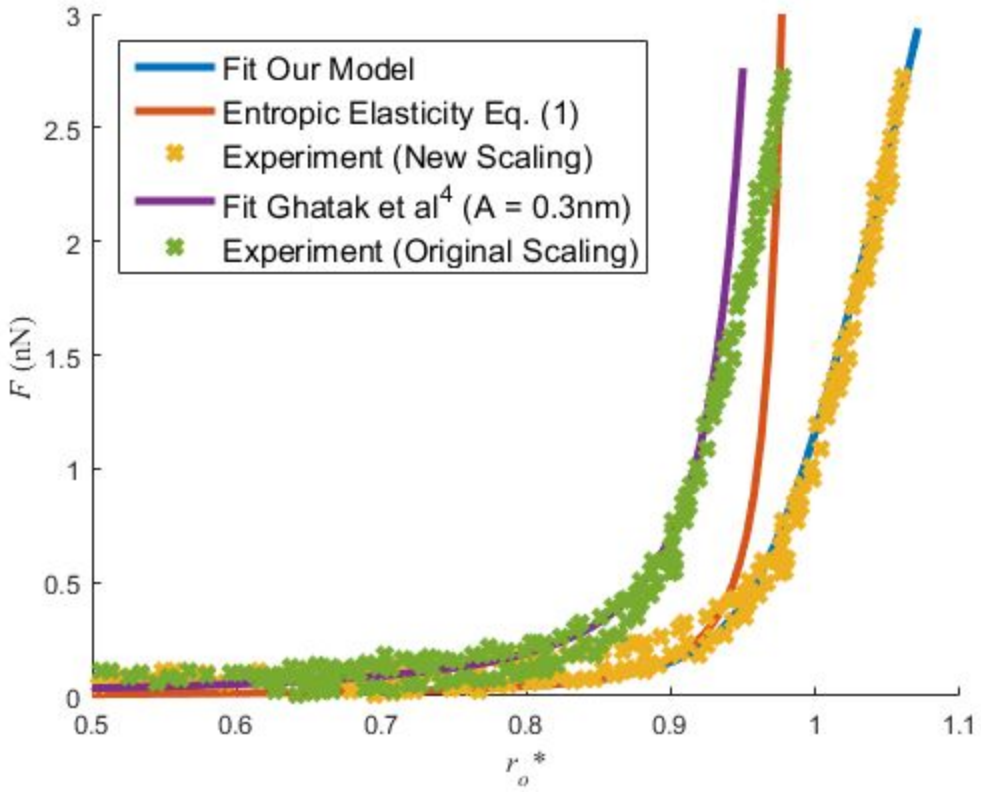

Figure 5: Comparison of the force-extension relationship from the entropic elasticity model Eq. (1), with the prediction by the model presented in this work and AFM experimental data for a single PDMS chain[4]. The parameters used in generating these graphs are for PDMS (Table 2) and Si-O bond (Table 1). Experimental data in Yellow correspond to scaling of the fractional extension by a factor of 1.085. Also shown are experimental data in Green without the scaling, and the fit provided in Ghatak et al[4] by using an entropic model and a small Kuhn length (0.3 nm).

3.2 Simple Chain with Bond Scission

To illustrate the scission of PDMS chains and its rate dependence, we calculate the surviving chain fraction b and the effective force F_{eff} for a number of extension rates (V) presented in Chaudhury[8], as shown in Figure 6. To generate these plots, the following parameter values are used: $k_o = 1 \times 10^{-13}$, $\Delta G^{\ddagger} = 1.125 \times 10^{-19} J$ and $x^{\ddagger} = 0.09 \times 10^{-9} m$. Here k_o and $x^{\ddagger}$ are close to the values used in the model of Chaudhury[8] while $\Delta G^{\ddagger}$ is chosen so that the

critical force (see Eq. (23)) would be close to the critical value reported in the literature[5]. It can be seen from the results that increasing the extension rate causes the damage to shift to higher fractional extensions (Figure 6a)); and this translates to an increase in the peak value of the effective force (Figure 6b)). At each extension rate, there exists a maximum extension at which b and F_{eff} reduce to zero. As the extension rate increases this maximum extension approaches an asymptotic limit (black dotted lines) because the forces on the bonds are approaching the critical force in Eq. (23). This is particularly evident in the purple curves in Figure 6 which correspond to the highest extension rate here.

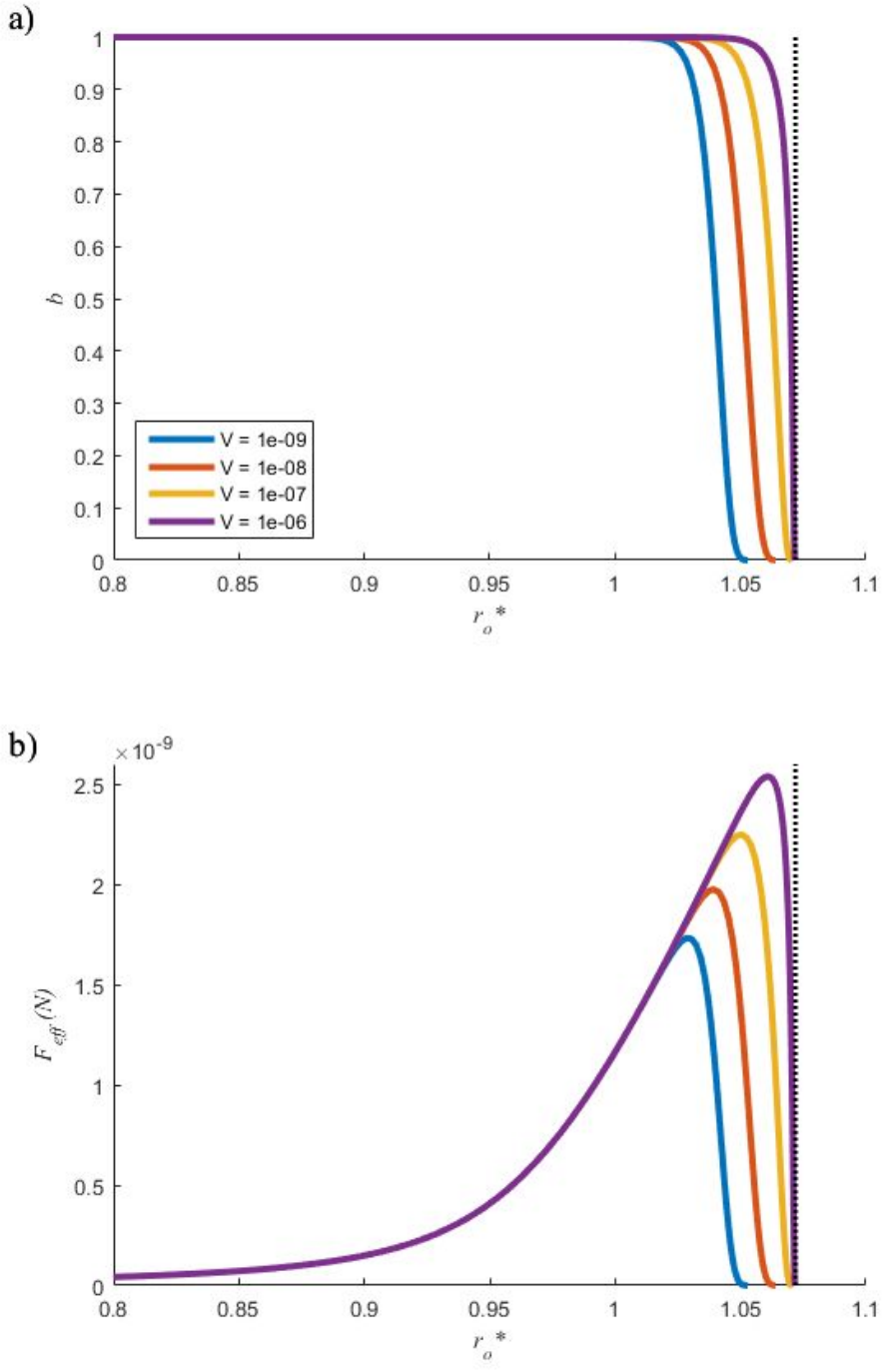

Figure 6 a) Surviving chain fraction, b, and b) Effective force F_{eff} = bF, plotted against fractional extension r_o for 4 different chain extension rates, V (m/s). The parameters used in generating these graphs are for PDMS (Table 2), Si-O bond (Table 1), temperature T = 298K, $k_o = 1 \times 10^{-13}$, $\Delta G^{\ddagger} = 1.125 \times 10^{-19} J$, and $x^{\ddagger} = 0.09 \times 10^{-9} m$.*

The model also allows us to determine the fracture energy of a PDMS interface (G), which can be computed as follows[1]

$$G = \int \Sigma F dr = N_K \Sigma_o k_B T \int b F^* dr_o^*, \quad (31)$$

where $F^* = FA_o/k_BT$ is the nondimensional polymer chain force, Σ is the areal density of load bearing polymer chains on the interface and Σ_o is the initial areal density of load bearing polymer chains prior to any applied load, i.e., $\Sigma = b\Sigma_o$. This fracture energy was measured as a function of interface separation speeds (V) in Chaudhury[8], and the experimental data (blue) are compared with predictions made by the model (red) in Figure 7. Here the contour length of the chain (L_c = 16.3 nm, equivalent to n_b = 129) and $\Sigma_o = 5.28 \times 10^{18} m^{-2}$ are parameters used to fit the experimental data. The model has reasonably reproduced the experimental data and captured the increased energy needed to rupture a polymeric interface at higher speed.

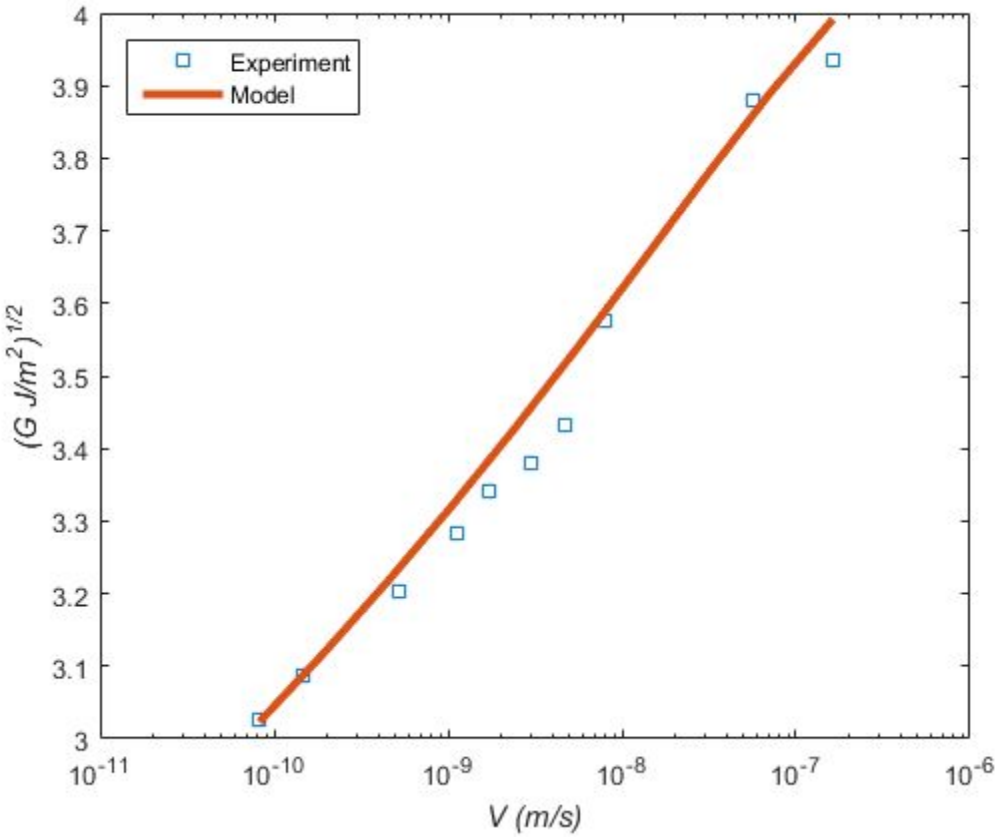

Figure 7: Frature energy $G^{1/2}$ plotted agaist interface spearation speed V. Experiemtnal data and model prediction are compared. The parameters used in generating these graphs are for PDMS (Table 2) and Si-O bond (Table 1). L_c = 16.3 nm and $\Sigma_o = 5.28 \times 10^{18} m^{-2}$ were found to provide a good fit to the experimental data.

3.3 Effect of Mechanophores on Chain Scission

Figure 8a) shows the surviving chain fraction for 3 PEA chains of different chain lengths (i.e., different number of Kuhn segments N_K) which do not contain any mechanophores. The corresponding effective force is shown in Figure 8b). Here a constant stretch rate of $\dot{\lambda} = 0.0171\ s^{-1}$ is applied in all cases, and Eqs. (24) and (27) can be transformed to eliminate time dependence under the constant rate (see Supporting Information Section S3 for details). Longer chains are observed to rupture at shorter extension since there are more bonds and hence more

potential failure points. Depending on the chain length, the peak of the effective force is between 2 and 3nN. The maximum extension, at which all bonds break, exceeds the entropic locking extension by 10-12%.

The same calculations are repeated for a polymer chain crosslinked with weaker mechanophore bonds, and the results are shown in Figure 9a) for b and in Figure 9b) for F_{eff}. In this example the mechanophores have dissociation energy of 150 kJ/mol, much lower than that of C-C bonds (350 kJ/mol)[12]. Because scission is now dominated by the rupture of mechanophores, the difference between different chain lengths is nearly negligible. Compared with the case without mechanophores (Figure 8) the peak force is less, between 1.5 and 2 nN; as well the maximum extension is reduced and only exceeds the entropic locking extension by about 5%.

Although the discussions here are for chains with mechanophores, an analogy can be drawn to crosslink failure in a polymer network which has recently been of interest[24,25] In particular, we can interpret mechanophores as crosslinks and allow two crosslinks per chain. For example, Ducrot et al.[12] studied the fracture of elastomeric networks crosslinked with bis(adamantly)-1,2-dioxetane bisacrylate, a photophore which has a bond weaker than the C-C backbone bonds and emits light when it is ruptured. The light emission observed at the crack tip implies that crosslink failure was taking place in the elastomer network, which leads to a small weakening effect on the toughness measurements. In our model, the relevant equations to account for crosslink rupture are Eqs. (24), (27) and (30). Eq (24) predicts the rate of rupture of backbone bonds of polymer chains, Eq. (27) with $n_0 = 2$ and $k_R = 0$ predicts the rate of rupture of crosslinks, and Eq. (30) specifies the surviving chain fraction due to both rupture of backbone bonds and crosslinks. In Figure 9, we see that the chain length dependence of the rupture force

mostly disappears since failure by mechanophores (and analogously by crosslinks) dominates. However, the computed rupture energy is proportional to the chain length since to calculate the energy from force, an integration similar to Eq. (6) will be performed.

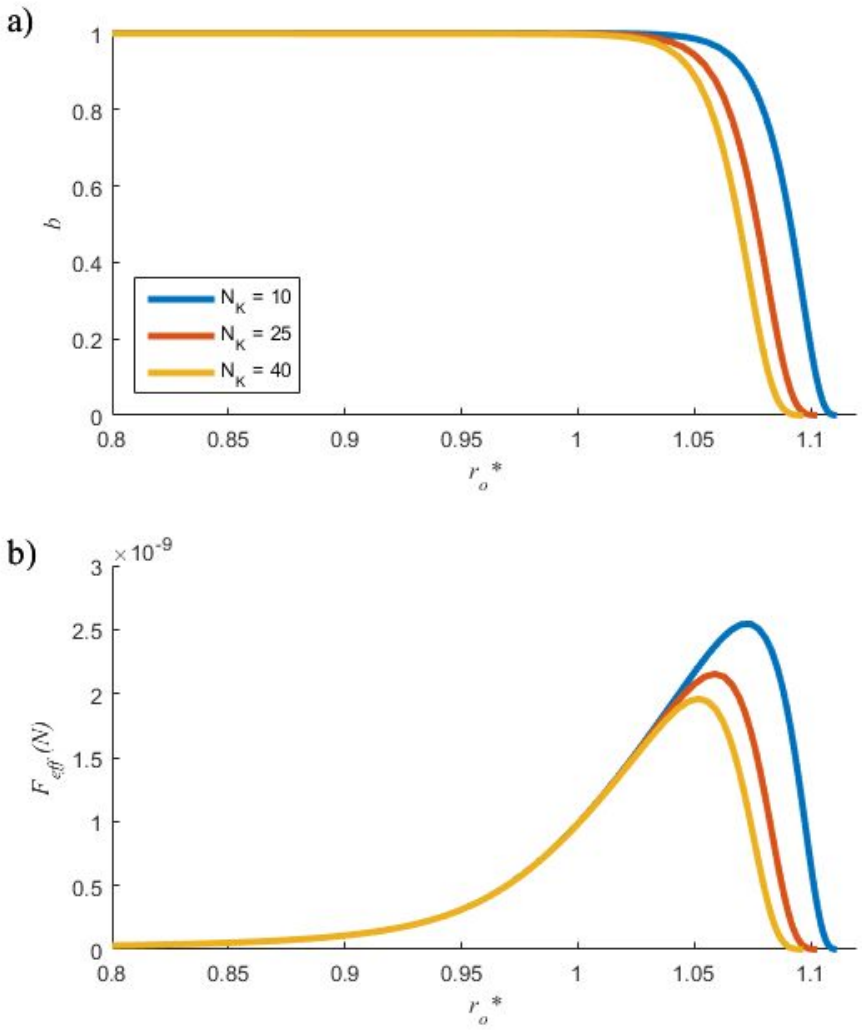

Figure 8 a) Surviving chain fraction, b, and b) Effective force F_{eff} = bF* =bFA_o/k_BT, plotted against fractional extension r_o* for 3 different chain lengths. The parameters used in generating these graphs are for PEA (Table 2), C-C bond (Table 1), temperature T = 298 K, stretch rate $\dot{\lambda} = 0.0171s^{-1}$, $k_o = 5 \times 10^{-9}$, $\Delta G^{\ddagger} = 40 \times 10^{-21}J$, and $x^{\ddagger} = 0.021 \times 10^{-9}m$. Because the values ($k_o$, $\Delta G^{\ddagger}$, $x^{\ddagger}$) for PEA are not available, they are chosen initially based upon the values in literature for PDMS[5], but have been adjusted to match experimentally measured stress in multinetwork elastomers (a model for multinetwork elastomer based on the chain model in this work is discussed by Lavoie[30]) .*

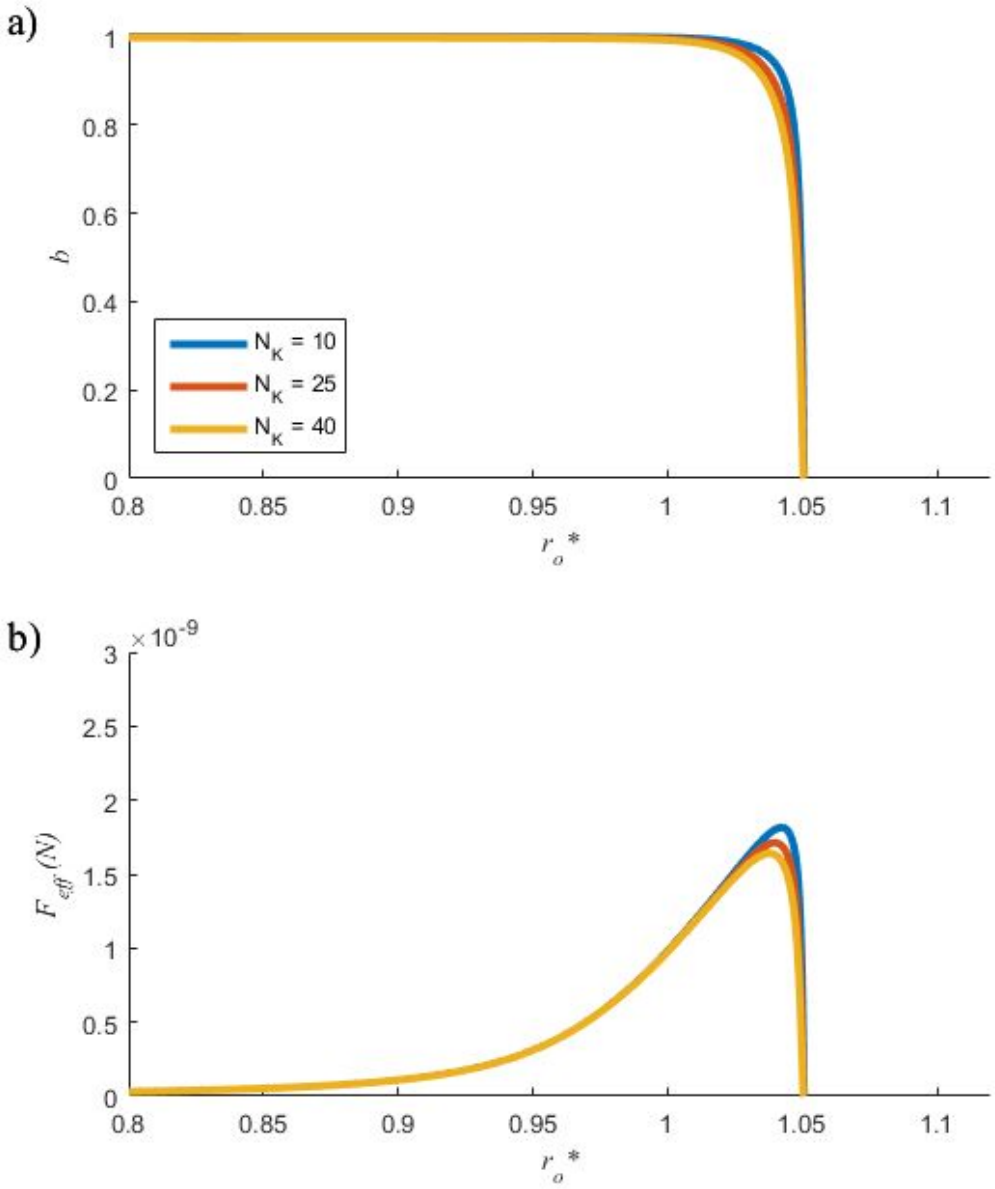

Figure 9 Results for the same polymer chains shown in Figure 8 but with a mechanophore on each end of the chains a) Surviving chain fraction, b, and b) Effective force F_{eff}, plotted against fractional extension r_o for 3 different chain lengths. The parameters used in generating these graphs are for PEA (Table 2), C-C bond (Table 1), temperature T = 298 K, and stretch rate* $\dot{\lambda} = 0.0171s^{-1}$. *The constants in reaction kinetics are* $k_o = 5 \times 10^{-9}$, $\Delta G^{\ddagger} = 40 \times 10^{-21}J$, *and* $x^{\ddagger} = 0.021 \times 10^{-9}m$ *for the regular bonds and* $k_o = 2 \times 10^{-6}$, $\Delta G^{\ddagger} = 20 \times 10^{-21}J$, *and* $x^{\ddagger} = 0.021 \times 10^{-9}m$ *for the mechanophores.*

3.4 Chains Composed of Mechanophores with Elongation Reaction

Finally we examine the situation where a polymer chain is composed entirely of mechanophore units that, upon activation, increase their length; it is assumed in this section that the bonds on the chains' backbones do not break. Using the potentials E_1 (syn-CL-gCFC) and E_2 (2-fluro-3-chloro-alkene (Z isomer)) from Wang et al.[13], the unreacted fraction b_{MP} and the predicted force F on a chain are plotted against r_o^* in Figure 10. In Figure 10a), b_{MP} initially stays at a constant value of 1 until the force, shown in Figure 10b), becomes sufficient for the mechanophores to react. Once this occurs b_{MP} drops smoothly to zero as all of the mechanophores react. The reaction of mechanophores increases the contour length of the polymer chain; therefore, larger increases in r_o^* are needed to increase the force. This creates a region in Figure 10b) where the increase of force with r_o^* significantly slows down. Experimental data from Wang et al.[13] is also shown in Figure 10b), which can be well fitted by the present model with $\Delta G^{\ddagger} = 32 \times 10^{-21} J$, $x^{\ddagger} = 0.025 nm$, $k_o = 8 \times 10^{-5} s^{-1}$ and $L_c = 745 nm$. The separation velocity in Wang et al.[13] was 300 nm/s, which corresponds to $dr_o^*/dt = 0.402$ used to generate Figure 10. Also shown for reference in Figure 10b) are the responses of a purely entropic chain, a 100% unreacted chain and a 100% reacted chain. The latter two can be calculated from the numerical solution of the reacting chain as follows. Once F_{MP} is known for the reacting chain Eqs. (20) and (1) are solved for r^* and F where the Kuhn length in Eq. (1) is replaced with

$$A_1 = \frac{n_b l \cos(\theta/2) + n_1 l_1}{N_K} \qquad (32)$$

for the 100% unreacted chain and

$$A_2 = \frac{n_b l \cos(\theta/2) + n_2 l_2}{N_K} \quad (33)$$

for the 100% reacted chain. In Figure 10b), the 100% unreacted chain (purple) matches the reacting chain (yellow) at low extensions (<0.95) and the 100% reacted chain (green) matches the reacting chain (yellow) at large extensions (>1.15). Between these extensions the reacting chain transitions between the two limits.

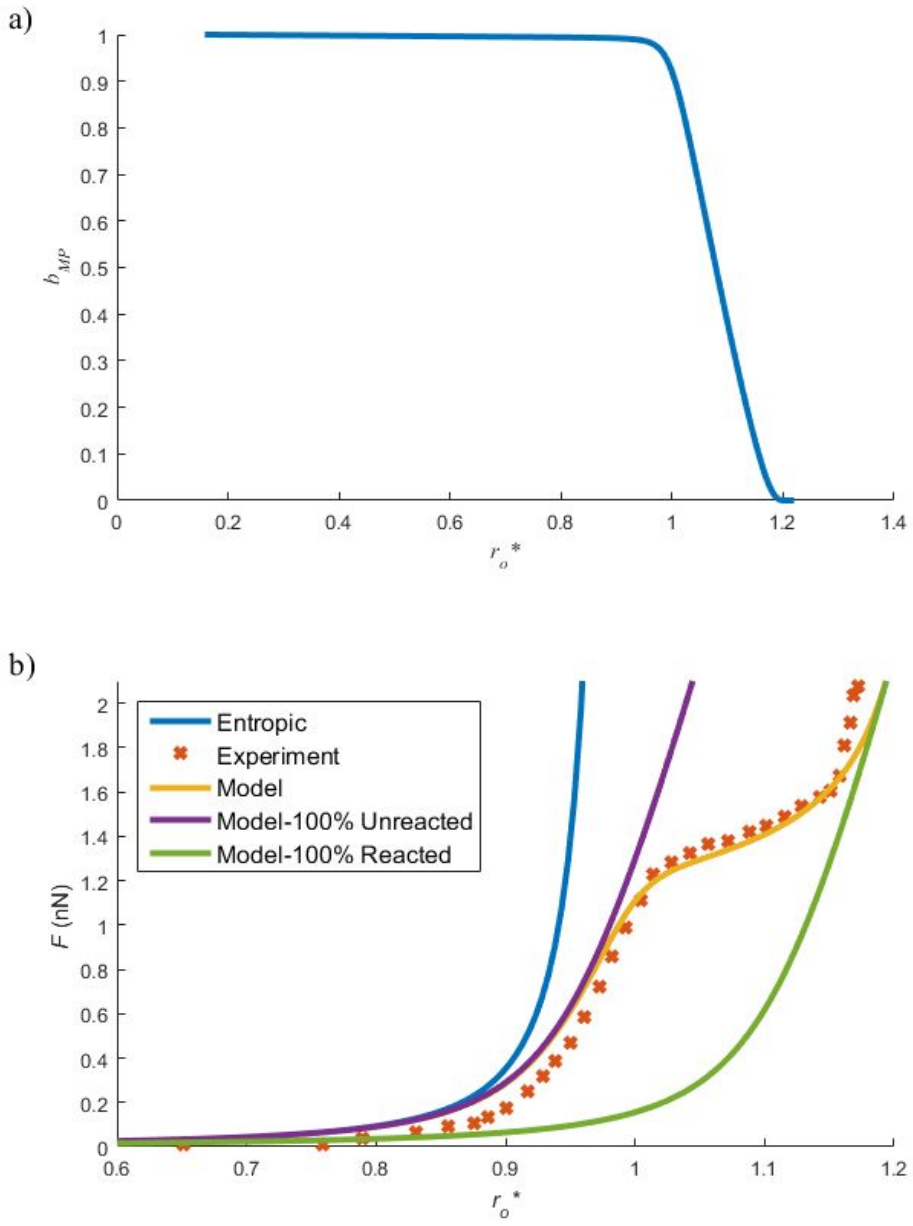

Figure 10: a) Unreacted mechanophore fraction vs r_o^*, b) Chain force vs r_o^*. Comparison is made between the force predicted by the model (yellow) and the experimental data[13] (red x). Also shown is the force predicted by using a purely entropic model (blue), by assuming all mechanophores are unreacted (purple), and by assuming all mechanophores are reacted (green). To generate this fit the potentials E_1 and E_2 (shown in Figure 3) from Wang et al.[13] were used. The parameters $\Delta G^{\ddagger} = 32 \times 10^{-21} J$, $x^{\ddagger} = 0.025nm$, $k_o = 8 \times 10^{-5} s^{-1}$ and $L_c = 745nm$ were used to obtain the fit.

The force-extension relationship, with a plateau, shown in Figure 10b) has the potential to be used to design elastomers with improved properties such as enhanced fracture toughness and ultimate stress. To illustrate this we will estimate the stress in a bulk material consisting of many chains of different number of Kuhn segments as was done in Lavoie et al.[3]. With the consideration of damage, the strain energy of the bulk polymer is given by

$$U = \nu_{ch}\int_1^\infty w(N_K) b E_{ch} dN_k, \quad (34)$$

where ν_{ch} is the volumetric density of polymer chains, b is the surviving chain fraction and $w(N_K)$ is a probability distribution function describing the number of chains which have N_K Kuhn segments. For the case of uniaxial extension the fractional extension can be related to macroscopic stretch λ according to the "8-chain" model[1]

$$r_o^* = \sqrt{(\lambda^2 + 2\lambda^{-1})/3N_K}, \quad (35)$$

and the stress can be written as [3]

$$\sigma = \mu\int_1^\infty w(N_K) \frac{b(r_o^*, N_K) F^*(r_o^*)}{3r_o^*} dN_K(\lambda^2 - \lambda^{-1}). \quad (36)$$

where $\mu = \nu_{ch} k_B T$ is the shear modulus when $r_o^* = 0$. An average surviving chain fraction which considers the weighted contribution of all chain lengths can be defined as follows[3]

$$b_t = \int_1^\infty w(N_K) b(r_o^*, N_K) dN_K. \quad (37)$$

For computation efficiency the curves in Figure 10b) are fitted with analytical functions and details of the fitting are given in the Supporting Information (Section S2).

Of particular interest is to compare how the different force-extension relationships will impact the stress. To investigate this we take three fitted force extension relationships from Figure 10b): an entropic chain, a reacting chain with reaction kinetics (elongating

mechanophores) and a 100% unreacted chain (no elongation caused by mechanophores). An identical relationship $b(F)$ for the surviving chain fraction is applied to all 3 cases (see Supporting Information Section S2 for details). The resulting non-dimensional effective forces, $F^*_{eff} = F_{eff}A_o/k_BT$ (see Eq. (28) for the definition of F_{eff}), are shown in Figure 11. In Figure 11, all curves are coincident until about $r_o^* = 0.9$ after which the entropic curve sharply increases due to chain inextensibility. The 100% unreacted and elongating mechanophore curves are coincident until about $r_o^* = 1$ when the elongation reaction begins. In all cases the mean break force[23] defined as

$$\langle F \rangle_b = \frac{k_BT}{A_o}\int_0^1 F^*\left(r_o^*\right)db \quad (38)$$

is the same because $b(F)$ is the same. The stress σ, normalized by μ, is plotted in Figure 12a) against the macroscopic stretch, and the average surviving chain fraction is shown in Figure 12b). For this figure $w(N_K)$ is assumed to be a uniform distribution. Comparing the three curves in Figure 12a) shows that the chain with reacting mechanophores lead to the largest stress followed by the chain with unreacting mechanophores, while the entropic chain produces the lowest stress. Similarly, chains with higher stress have higher surviving chain fraction in Figure 12b). The ability for the chain to prevent failure by increases in length allows more chains, of different lengths, to have higher force at any given stretch, which increases the maximum stress. To quantify this effect we define a force efficiency as

$$\eta_F = \frac{\langle F_{eff}\rangle_{N_K}}{\langle F\rangle_b} = \frac{\int_1^\infty w(N_K)b\left(r_o^*,N_K\right)F^*\left(r_o^*\right)dN_K}{\int_0^1 F^*\left(r_o^*\right)db}, \quad (39)$$

where the numerator is an average force considering the contributions from chains of different number of Kuhn segments (N_K):

$$\langle F_{eff}\rangle_{N_K} = \frac{k_B T}{A_o}\int_1^{\infty} w(N_K) b(r_o^*, N_K) F^*(r_o^*) dN_K. \quad (40)$$

The magnitude of the force efficiency provides a direct measure of how well the elastomer is able to distribute load between all chains. A peak efficiency near one means that the elastomer is able to engage all chains with maximum force simultaneously when it achieves peak stress while an efficiency near zero means that few chains will have maximum force in the material at any time. The force efficiencies for the three types of polymers in Figure 11 are plotted in Figure 12c) and correlates well with the stress in Figure 12a).

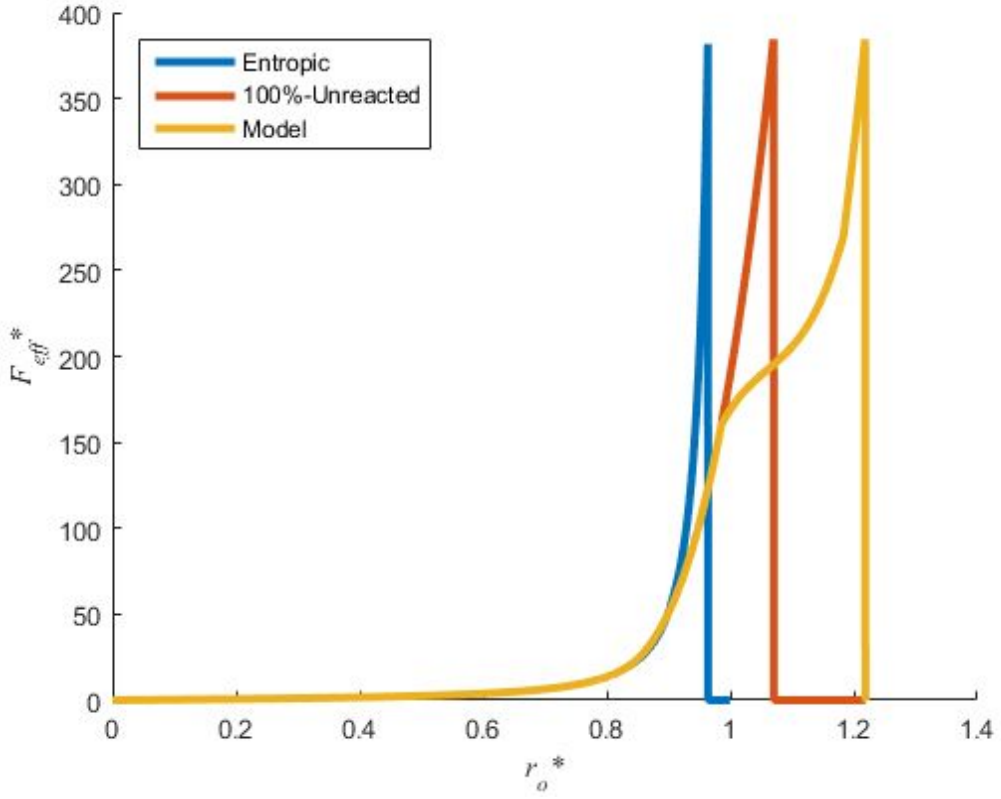

Figure 11: Non-dimensional effective force $F_{eff}^* = bF^* = bFA_o/k_BT$ plotted against fractional extension r_o^* for 3 different chain models: a fully entropic chain, a chain where the mechanophores do not react and a chain where mechanophores can react. The same relation $b(F)$ for the surviving chain fraction is applied to each case.

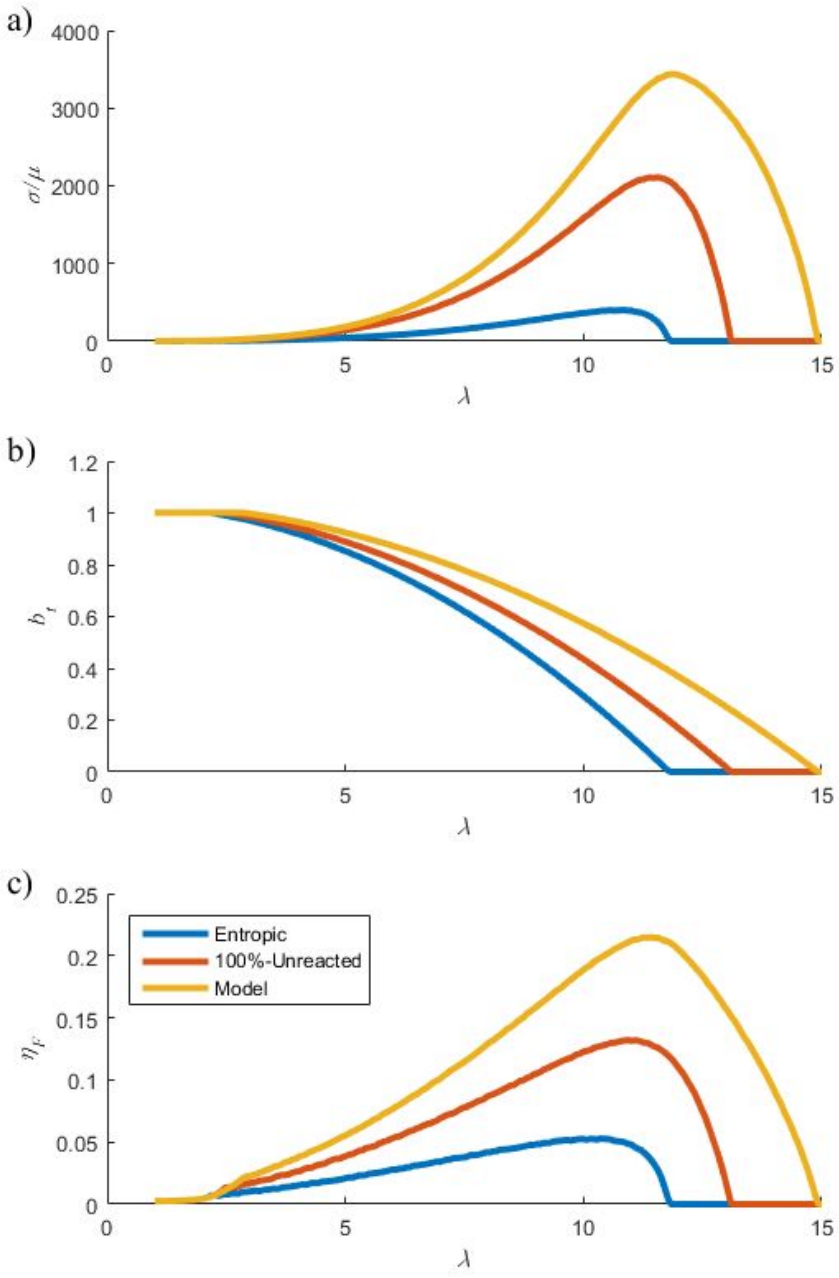

Figure 12 a) Nondimensional stress vs. stretch b) Surviving chain fraction vs. stretch c) Force efficiency vs. stretch. In each subfigure three curves are shown each corresponding to a different chain model from Figure 11. $w(N_K)$ *has been chosen to be a uniform distribution from* $N_K = 2 - 50$.

A few comments are warranted to put Figure 12 into perspective. Firstly, Figure 12a) suggests that the stress can be three orders of magnitude larger than μ which far exceeds anything that has been observed. For example for the single network elastomers presented in Ducrot et al[12] the true stress at break is of the same order of magnitude as the Young's modulus; whereas data for latex rubber show a true stress at break that is two orders of magnitude greater than μ[27]. The discrepancy in magnitude is most likely due to the fact that real materials contain defects, which lead to stress concentrations, localized damage, and failure much earlier than what is shown in Figure 12a). If a stress concentration is present in the experiments, the maximum local stress may be much higher than the maximum measured stress because this large stress only occupies a small fraction of the materials volume. Furthermore, the effect of the nonlinear force-extension relationship often cannot be fully reflected in experimental data for elastomers. For example in the single network data presented in Ducrot et al[12], only a small fraction of the material's volume has chains subjected to high force when the sample fails. In these types of brittle elastomers designing the material with special polymer chains is unlikely to yield a significant improvement in properties. However, special manufacturing techniques have been used to dramatically enhance the toughness of brittle elastomers[12]. In multinetwork elastomers the first network (filler network) is prestretched by introducing additional networks (matrix networks). Prestretched chains can break while the matrix networks prevent large crack from forming[12]. In this type of material, it stands to reason that using special polymer chains in the filler network could lead to a significant enhancement to the maximum stress and toughness.

4 Conclusion

A model is developed to predict force-extension relationships for polymer chains by minimizing the free energy containing contributions from configurational entropy and energies for backbone bond deformation. Parameters in this model are largely molecular parameters available in the literature, and hence the number of parameters needed from fitting experimental data is minimal. Compared with classical entropic chain models the force-extension relationship is significantly softer at large extension, owing to the ability of the bonds to deform. The model is subsequently extended to include the consideration of active polymer chains containing mechanophores. The model is able to reproduce the rate dependent fracture energy needed to advance a crack in PDMS, as well as the plateau in force-extension relationship caused by mechanophores that increase the contour length of the chain when subjected to sufficient tensile force. By implementing the force-extension relationship developed here into a simple constitutive model, it is shown that this type of active chain has the potential to significantly improve the maximum stress and toughness that elastomers can achieve.

5 Supporting Information

- Alternative entropic chain energies
- Fitted functions for the force-extension relationship
- Rate of chain extension under uniaxial loading

6 Acknowledgement

The authors acknowledge financial support from the Natural Science and Engineering Research Council (NSERC), Canada Foundation for Innovation and Alberta Innovates

Technology Futures. R.L. acknowledges the support from a National Science Foundation CAREER award (CMMI-1752449).

7 Nomenclature

A_o	Initial Kuhn length
A	Kuhn length
A_1, A_2	Kuhn length of unreacted and reacted mechanophore units respectively
b	Surviving chain fraction
b_t	Average surviving chain fraction
b_P	Surviving regular bonds
b_{MP}	unreacted fraction of mechanophores
$\underline{\boldsymbol{B}}$	Left Cauchy Green deformation tensor
β_s	Constant which controls width of Morse potential
C_∞	Asymptotic value of Flory's characteristic ratio
D_e	Bond dissociation energy
E_{ch}	Energy of polymer chain
E_{ent}	Entropic component of polymer chain energy
E_{str}	Energy of stretching a single bond on the backbone
E_{ben}	Energy of deforming a single bond angle on the backbone
E_1, E_2	Energy of one unreacted and reacted mechanophore units respectively
F	Tensile force acting on a polymer chain
F^*	Nondimensional polymer chain force ($F^* = FA_o/k_BT$)
F_{eff}	Effective tensile force on a polymer chain with consideration of bond rupture
F^*_{eff}	Nondimensional effective force ($F^*_{eff} = F_{eff}A_o/k_BT$)
F_{pk}	Maximum bond force possible in Morse potential
F_{str}	Tensile force acting on individual bonds in the chain
F_{MP}	Force acting on the mechanophore units
F_1, F_2	Force acting on unreacted and reacted mechanophore units respectively
f	Mechanical force
f_{crit}	Critical force
$\langle F \rangle_b$	Mean break force
$\langle F_{eff} \rangle_{N_K}$	Chain length averaged effective force
$\Delta G^\ddagger$	activation energy of the transition state
G	Fracture Energy
$I_1(\underline{\boldsymbol{B}})$	1st invariant of the left Cauchy Green deformation tensor of the bulk polymer
k_B	Boltzmann Constant
k_θ, k_s	Bending constants
k	Reaction rate
k_o	Reaction rate constant
λ	Stretch in uniaxial extension
$\dot{\lambda}$	Rate of stretch in uniaxial extension
l_o	Initial bond length
l	Bond length
L_c	Contour length of a polymer chain

l_{pk}	Bond length for peak force in Morse potential
l_1, l_2	Bond length of unreacted and reacted mechanophore units respectively
M	Bending moment acting on bonds
M_b	Average molecular weight per backbone bond
M_{ch}	Molecular weight of a chain
M_K	Molecular weight of a Kuhn segment
M_m	Molecular weight of a single monomer (repeating unit in the polymer)
n_b	Number of backbone bonds on polymer chain
n_m	Number of backbone bonds in one repeating monomer unit
n_0	$n_0 = n_1(t = 0)$
n_1, n_2	Number of mechanophore units in unreacted and reacted states respectively
P	Persistence length of polymer chain
θ_o	Initial bond angle
θ	Bond angle
ρ	Mass density of polymer
r	Polymer chain end-to-end distance
r^*	Fractional extension of polymer chain, with reference to current contour length
r_o^*	Fractional extension of polymer chain, with reference to initial contour length
$\langle R_o^2 \rangle$	Mean square end-to-end distance of free polymer chain (before application of external load)
σ	Cauchy stress
Σ	areal density of load bearing polymer chains
Σ_o	initial areal density of load bearing polymer chains prior to any applied load
T	Temperature
t	Time
U	strain energy density
V	Extension Rate
υ_{ch}	Volumetric density of polymer chains
w	probability distribution function describing the number of chains which have N_K Kuhn segments
$x^{\ddagger}$	activation length of the transition state
ξ	Ratio of number of bonds to number of Kuhn segments per chain
η_F	Force efficiency
μ	Shear modulus

8 References

(1) Arruda, E.M, Boyce, M.C. A Three-dimensional constitutive model for the large stretch behavior of rubber elastic materials, *J. Mech. Phys. Solids.*, **1993**, 41, 389-412

(2) Dobrynin, A.V., Carrillo, J.M Y., Rubenstein, M. Chains are more flexible under tension, *Macromolecules*, **2010**, 43, 9181-9190

(3) Lavoie, S.R.; Long, R.; Tang, T. A rate dependent damage model for elastomers at large strain, *Extreme Mech. Lett*., **2016**, 8, 115-124

(4) Ghatak, A.; Vorvolakos, K.; She, H.; Malotky, D.L.; Chaudhury, M.K. Interfacial rate processes in adhesion and friction, *J. Phys. Chem. B.*, **2000**, 104, 4018–4030

(5) Schwaderer, P.; Funk, E.; Achenbach, F.; Wies, J.; Brauchle, C.; Michaelis, J. Single molecule measurement of the strength of a siloxane bond, *Langmuir*, **2008**, 24, 1343-1349

(6) Mao, Y.; Talamini, T.; Anand, L. Rupture of polymers by chain scission E*xtreme Mechanics Letters*, **2017**, 13, 17-24

(7) Talamini, T.; Mao, Y.; Anand, L. Progressive damage and rupture in polymers, *J. Mech. Phys. Solids*, **2018**, 111, 434-457

(8) Chaudhury, M.K. Rate-dependent fracture at adhesive interface, *J. Phys. Chem. B.*, **1999**, 103, 6562–6566

(9) Hui, C.Y.; Tang, T.; Lin, Y.Y.; Chaudhury, M.K. Failure of elastomeric polymers due to rate dependent bond rupture, *Langmuir*, **2004**, 20, 6052–6064

(10) Wang, Q.; Gossweiler, G.R.; Craig, S. L; Zhao, X. Mechanics of mechanochemically responsive elastomers, *J. Mech. Phys. Solids,* **2015**, 82, 320-344

(11) Silberstein, M.N.; Cremar, L.D.; Beiermann, B. A; Kramer, S.B.; Martinez, T.J.; White, S.R.; Sottos, N.R. Modeling mechanophore activation within a viscous rubbery network, *J. Mech. Phys. Solids,* **2014**, 63, 141-153

(12) Ducrot, E., Chen, Y., Butlers, M., Sijbesma, R.P., Creton, C. Toughening elastomers with sacrificial bonds and watching them break, *Science,* **2014**, 344, 186-189

(13) Wang, J.; Kouznetsova, T.B.; Craig, S. Reactivity and mechanism of a mechanically activated anti-Woodward-Hoffmann-DePuy reaction, *J. Am.Chem. Soc,* **2015**, 137, 11554-11557

(14) Wang, J.; Kouznetsova, T.B.; Niu, Z.; Ong, M.T.; Klukovich, H.M.; Rheingold, A.L.; Martinez, T.J.; Craig, S. L. Inducing and quantifying forbidden reactivity with single molecule polymer mechanochemistry, *Nature Chemistry,* **2015**, 7, 323-327

(15) Brown, C.L.; Craig, S. L. Molecular Engineering of mechanophore activity for stress-responsive polymeric materials, *Chem. Sci.,* **2015**, 6, 2158-5165

(16) Wu, D.; Lenhardt, J.M.; Black, A.L.; Akhremitchev, B. B.; Craig, S. L. Molecular stress relief through a force-induced irreversible extension in polymer contour length, *J. Am.Chem. Soc.,* **2010**, 132, 15936-15938

(17) Wang, J.; Kouznetsova, T.B.; Boulatov, R.; Craig, S. L. Mechanical gating of a mechanochemical reaction cascade, *Nature Communications,* **2016**, 7, 13433

(18) Rubenstein, M., Colby, R.H. Polymer Physics. 2003, Oxford University Press

(19) Aklonis, J.J; MacKnight, W.J. Introduction to polymer viscoelasticity, 2nd edition, 1983, John Wiley and Sons, New York

(20) Awang, M.; Mohammadpour, M.; Muhammad, I.D. Finite element modeling of nanotube structures linear and non-linear models, 2016, Springer, Chapter 2

(21) Stixrude, L.; Bukowinski, M.S.T. Simple covalent potential models of tetrahedral SiO2 applications to a-quartz and coesite at pressure, *Phys Chem Minerals*, **1988**, 16, 199-206

(22) Mark, J.E. Physical properties of polymers handbook, 2nd Edition, Springer, 2007, Chapter 25

(23) Dudko, O.; Hummer, G.; Szabo, A. Intrinsic rates and activation free energies from single molecule pulling experiments, *Physical Review Letter*, **2006,** 96, 108101

(24) Mao, Y.; Anand, L. Fracture of elastomeric materials by crosslink failure, *J. Appl. Mech.*, **2018**, 85, 081008

(25) Raayai-Ardakani, S.; Earl, D. R., Cohen, T. The intimate relationship between cavitation and fracture, *Soft Matter,* **2019**, 15, 4999

(26) Press, W.H.; Teukolsky, S.A., Vetterling, W.T.; Flannery, B.T. *Numerical Recipes The Art of Scientific Computing 3rd Ed*., Cambridge University Press, Cambridge, 2007

(27) Treloar, L.R.G. Stress-Strain data for vulcanized rubber under various types of deformation, *Trans. Faraday Soc.,* **1944**, 40, 59-70

(28) Lake, G.J.; Thomas, A.G. The strength of highly elastic materials, *Proc. R. Soc. Lond. A*, **1967**, 300, 108-119

(29) Lavoie, S.R., Long, R., Tang, T. An adhesive zone model for polymeric interfaces, *Int. J. Fracture*, **2016**, 197, 169-183

(30) Lavoie, S.R. PhD Thesis, University of Alberta, 2018